

**Model calculation of the electron-phonon coupling in Cs/Cu(111)**Akihiro Nojima,<sup>1</sup> Koichi Yamashita,<sup>1</sup> and Bo Hellsing<sup>2,3</sup><sup>1</sup>*Department of Chemical System Engineering, School of Engineering, The University of Tokyo, Hongo 7-3-1, Bunkyo-ku, Tokyo 113-8656, Japan*<sup>2</sup>*Department of Physics, Göteborg University, Fysikgränd 3, S-412 96 Göteborg, Sweden*<sup>3</sup>*Donostia International Physics Center (DIPC), Paseo de Manuel Lardizabal, 4, 20018 San Sebastian/Donostia, Spain*

(Received 20 March 2008; revised manuscript received 22 May 2008; published 10 July 2008)

A simplified calculation scheme is proposed for the analysis of the phonon-induced lifetime broadening of surface-electronic states. The aim has been to include the details of the electron and phonon structures. In contrast to the present analysis based on phonon Debye models, where all is hidden in the parameters Debye frequency  $\omega_D$  and electron-phonon coupling constant  $\lambda$ , our procedure gives a single multiplicative fitting parameter  $V_d^2$  for the spectral Eliashberg function, where  $V_d$  represents the effective deformation potential. We apply this procedure to the image and surface states of Cu(111) and to the quantum-well state and the recently found gap state of  $p(2 \times 2)$ -Cs/Cu(111). We demonstrate that the crucial contribution to the electron-phonon coupling by the overlayer localized low-frequency phonon modes is well captured by the scheme. The presented scheme should be useful for combined experimental and theoretical studies of overlayer systems for which still no full *first-principles* calculation of the electron-phonon coupling has been presented due to the complexity of the system.

DOI: [10.1103/PhysRevB.78.035417](https://doi.org/10.1103/PhysRevB.78.035417)

PACS number(s): 73.20.At, 73.50.Gr, 73.21.Fg, 82.45.Mp

**I. INTRODUCTION**

The characterization and understanding of adsorption and reactivity of alkali metals on metal surfaces have for several decades been central issues in surface science. These systems can today be considered as atomically controllable prototypes of many catalytic reactions and surface functionalizations.<sup>1</sup> Moreover, lately the electronic structure and in particular, the electron dynamics has been the subject of detailed investigations of these systems. In this context, the quantum-well states (QWSs), formed in ultrathin alkali metal over layers on metal surfaces are of particular interest.<sup>2-11</sup> The QWS is a well-defined state hosting quantum-mechanically confined electrons in the dimension normal to the surface. These states have attracted much attention, not only due to the fact that they give us the possibility to study fundamental processes, e.g., the electron-phonon (EP) coupling, but also due to the possible applications in the field of nanoscale devices. From an experimental point of view, photoemission spectroscopy (PES) and scanning tunneling spectroscopy (STS) have made it possible to resolve details of the electron-scattering processes.<sup>6,10-12</sup>

Information of the dynamical decay process, following the creation of a QWS photohole in PES can be obtained from line-shape analysis.<sup>6,11</sup> For example, the linear increase of the line width is a fingerprint of a phonon-assisted decay channel. Recently, QWS lifetimes has also been studied with STS.<sup>10,12</sup> One of the advantages with this technique is the possibility to study by scanning tunneling microscopy (STM), local regions of the surface, where the atomic structure is suitable before the STS measurement is performed. For the understanding of the mechanisms that determines lifetimes of excited states, theoretical investigations are indispensable.

For an estimate of the phonon-induced contribution to the lifetime broadening, a phonon-Debye model typically gives

the correct order of magnitude.<sup>6,10-12</sup> However, as the microscopic ingredients are left out, such as, e.g., surface-phonon modes, we cannot make any link between experimental data and calculated details of the electron and phonon structures. Furthermore, for alkali overlayer systems, which are the focus of this investigation, a change of the alkali atom coverage strongly influences the phonon structure. This has been pointed out in several previous theoretical and experimental studies.<sup>13-18</sup>

However, *first-principles* studies<sup>19-24</sup> are still very demanding for these systems, which call for approximative methods that retain the main properties of the electronic and phonon structures of the system. In the present work, we present a simplified calculation scheme for the Eliashberg spectral function (ESF). With ESF, we calculate the phonon-induced lifetime broadening of surface-localized electronic states. The scheme takes into account (i) the basic features of the particular electronic state in terms of its wave function and (ii) the phonon structure, including dispersion relation and polarization fields. We apply this method to calculate the lifetime of the surface state (SS) and image state (IS) of Cu(111), and the QWS and the recently found gap state (GS) of  $p(2 \times 2)$ -Cs/Cu(111).

A recent density functional theory (DFT) study of  $p(2 \times 2)$ -Cs/Cu(111) shows the existence of an electronic state in the projected bulk band gap with a band energy of 0.9 eV above the vacuum level in the  $\bar{\Gamma}$  point.<sup>25</sup> The wave function of GS is strongly localized within the Cs layer and has a large in-surface plane kinetic energy. One proposed application of this state is in the field of electron-induced surface reactions.<sup>25</sup> Because of a zero elastic width, we expect that the inherent width will be determined by electron-electron (EE) and EP scattering. For this reason, we have also applied our scheme to calculate the EP-coupling-induced lifetime broadening of this state.

The paper is organized as follows: In the theory section (Sec. I), we give a rather detailed outline of our approxima-

tion of the Eliashberg function. As the focus of the work is to motivate a simplification in the calculation of the Eliashberg function, we give most of the details, except the renormalization of the phonon-polarization field, which is put in the Appendix. The calculation section (Sec. II) then follows, which gives the input, model electron and phonon structures. Results of the phonon-induced lifetime broadening of several surface-localized electronic states are presented in the lifetime broadening section (Sec. III). The paper ends with a summary (Sec. IV).

## II. THEORY

The general expression for the phonon-induced lifetime broadening of a SS, characterized by the binding energy  $\varepsilon_b$  and wave function  $|ss\rangle$  is<sup>26,27</sup>

$$\Gamma = 2\pi\hbar \int_0^\infty \alpha^2 F(\omega) [1 + 2n(\omega; T) + f(-\varepsilon_b + \omega; T) - f(-\varepsilon_b - \omega; T)] d\omega, \quad (1)$$

which gives for zero temperature ( $T=0$ ),

$$\Gamma_0 = 2\pi\hbar \int_0^\infty \alpha^2 F(\omega) d\omega, \quad (2)$$

where  $f$  and  $n$  are the electron and phonon distribution functions. The ESF is given by

$$\alpha^2 F(\omega) = \sum_{\nu, \vec{q}, \vec{k}} |g_{\nu, \vec{q}}^{\vec{k}}|^2 \delta(\omega - \omega_{\nu, \vec{q}}) \delta(\varepsilon_{ss} - \varepsilon_{\vec{k}}), \quad (3)$$

thus the cutoff of the frequency integrations in Eqs. (1) and (2) is determined by the cutoff of the phonon spectrum. The EP coupling function  $g$  is given by

$$g_{\nu, \vec{q}}^{\vec{k}} = \sum_j \sqrt{\frac{\hbar}{2NM_j\omega_{\nu, \vec{q}}}} \langle ss | \vec{\varepsilon}_{\nu, \vec{q}} \cdot \vec{\nabla}_{\vec{R}} V | \vec{k} \rangle, \quad (4)$$

where  $N$  is the number of the ions,  $j$  is the ion index, and  $\vec{R}$  is the ion coordinate.  $\vec{\varepsilon}_{\nu, \vec{q}}$  is the phonon-polarization vector field of the phonon mode  $\nu$  with wave vector  $\vec{q} = \vec{k}_{ss} - \vec{k}$ .

From photoemission experiments, information of the low-temperature strength of the EP coupling can be obtained from measurements at high temperatures  $\hbar\omega \ll k_B T$ . Then the line width is linear with temperature

$$\Gamma = 2\pi\lambda_0 k_B T, \quad (5)$$

where the low-temperature EP coupling parameter  $\lambda_0$  is given by

$$\lambda_0 = 2 \int_0^\infty \frac{\alpha^2 F(\omega)}{\omega} d\omega. \quad (6)$$

If we estimate  $\Gamma_0$  using the three-dimensional (3D) Debye model, then ESF is given by  $\lambda_0(\omega/\omega_D)^2$ , we obtain by applying Eq. (2)

$$\Gamma_0 = \frac{2}{3} \pi \lambda_0 \hbar \omega_D. \quad (7)$$

However in this estimate, which typically is based on an experimentally determined  $\lambda_0$  and a bulk Debye frequency  $\omega_D$ , all the physics is buried in these two parameters. Thus we learn nothing about how the detailed electron and phonon structures of the system influence the lifetime. This conclusion essentially holds, even if we refine our modeling with the two-dimensional (2D) or  $2D+3D$  phonon Debye models.<sup>27</sup>

In particular, which will be demonstrated in this paper, surface-phonon modes play a crucial role for the structure of the ESF, and in turn also for the lifetime.

We now return to the general expression for ESF in Eq. (3). Applying the quasistatic approximation  $\varepsilon_{ss} \simeq \varepsilon_{\vec{k}}$ , we sum up the overall initial electronic states  $\vec{k}$ .

$$\begin{aligned} \alpha^2 F(\omega) &= \sum_{\nu, \vec{q}, \vec{k}} |g_{\nu, \vec{q}}^{\vec{k}}|^2 \delta(\omega - \omega_{\nu, \vec{q}}) \\ &= \sum_{\nu, \vec{q}} \sum_{\vec{k}} \langle ss | A_{\nu, \vec{q}} | \vec{k} \rangle \langle \vec{k} | A_{\nu, \vec{q}}^\dagger | ss \rangle \delta(\omega - \omega_{\nu, \vec{q}}), \end{aligned} \quad (8)$$

where

$$A_{\nu, \vec{q}} = \sum_l \sqrt{\frac{\hbar}{2N_l M_l \omega_{\nu, \vec{q}}}} \sum_j \vec{\varepsilon}_{\nu, \vec{q}}(l, j) \cdot \vec{\nabla}_{\vec{R}} V(l, j; \vec{r}), \quad (9)$$

where we have in mind a slab calculation with slab layers labeled with indices  $l$  and  $j$  denoting the atoms in the layer. For the time being, we suppress the layer index and let index  $j$  labels any atomic position.

We now make the basic approximation of our proposed simplified scheme, namely, that the  $\vec{k}$  states form a complete set within the local volumes of integration, determined by the local character of the deformation potential.

$$\sum_{\vec{k}} \langle \vec{r} | \vec{k} \rangle \langle \vec{k} | \vec{r}' \rangle \approx \delta(\vec{r} - \vec{r}'). \quad (10)$$

We then have

$$\alpha^2 F(\omega) = \sum_{\nu, \vec{q}} B_{\nu, \vec{q}} \delta(\omega - \omega_{\nu, \vec{q}}), \quad (11)$$

where

$$B_{\nu, \vec{q}} = \frac{\hbar^2}{2N\omega_{\nu, \vec{q}}} \sum_{j, j'} \frac{1}{\sqrt{M_j M_{j'}}} T_{\nu, \vec{q}}(j, j'). \quad (12)$$

In this expression,  $T$  is given by

$$T_{\nu, \vec{q}}(j, j') = \langle ss | D_{j, \nu, \vec{q}}(\vec{r}) D_{j', \nu, \vec{q}}^*(\vec{r}) | ss \rangle, \quad (13)$$

where  $D$  carries the information of the scalar product of the phonon-polarization fields and the gradient of the screened ion-electron potential,

$$D_{j, \nu, \vec{q}}(\vec{r}) = \vec{\varepsilon}_{\nu, \vec{q}}(j) \cdot \vec{\nabla}_{\vec{R}} V(\vec{R}, j; \vec{r}). \quad (14)$$

Now  $\vec{\nabla}_{\vec{R}} V(\vec{R}, j; \vec{r})$  is different from zero, only in a small volume near equilibrium position of the ion.<sup>26-28</sup> The range

of this volume is typically confined within half the distance to the nearest-neighbor lattice site.<sup>28</sup> Thus the  $T$  matrix in Eq. (13) is symmetric ( $j=j'$ ). Applying the rigid ion approximation (RIA), we have

$$\vec{\nabla}_{\vec{R}} V(\vec{R}_j, \vec{r}) \approx \vec{\nabla}_{\vec{R}} V(\vec{R}_j - \vec{r}) = -\vec{\nabla}_{\vec{r}} V(\vec{R}_j - \vec{r}), \quad (15)$$

where  $\vec{r}=(x, y, z)$  is the electron coordinate. The anisotropy of the deformation potential, with respect to  $x$ ,  $y$ , and  $z$  has to be taken into account. In order to reduce the number of parameters to a single one  $V_d$ , we introduce the renormalized polarization vector (see Appendix),

$$\vec{\varepsilon}(\nu\vec{q}) = [\tilde{\varepsilon}_x(\nu\vec{q}), \tilde{\varepsilon}_y(\nu\vec{q}), \varepsilon_z(\nu\vec{q})], \quad (16)$$

Turning back to Eqs. (9)–(13), we have

$$\begin{aligned} & \sum_{l,j,\vec{k}} \langle ss | \vec{\varepsilon}(l,j) \cdot \vec{\nabla} V(\vec{k}) \langle \vec{k} | \vec{\varepsilon}^*(l,j) \cdot \vec{\nabla} V | ss \rangle \\ & \approx \langle ss | \sum_{l,j} \sum_{\alpha} \tilde{\varepsilon}_{\alpha}(l,j) \frac{\partial V}{\partial z} \sum_{\beta} \tilde{\varepsilon}_{\beta}^*(l,j) \frac{\partial V}{\partial z} | ss \rangle \\ & = \langle ss | \left( \frac{\partial V}{\partial z} \right)^2 \sum_{l,j} \sum_{\alpha} \tilde{\varepsilon}_{\alpha}(l,j) \sum_{\beta} \tilde{\varepsilon}_{\beta}^*(l,j) | ss \rangle \\ & = V_d^2 \sum_{l,j} I_l \tilde{\varepsilon}(l,j) \otimes \tilde{\varepsilon}^*(l,j), \end{aligned} \quad (17)$$

where  $\otimes$  denotes dyad product and

$$I_l = \int_{z_{l+1}}^{z_l} |\phi_{ss}(z)|^2 dz, \quad (18)$$

where  $z_l$  is located in the middle between the layer  $l$  and  $l+1$ . Then  $B_{\nu,\vec{q}}$  which is inserted in Eq. (11), now explicitly indicating the atom index  $j$  in layer  $l$  is given by

$$B_{\nu,\vec{q}} = V_d^2 \frac{\hbar^2}{2\omega_{\nu,\vec{q}}} \sum_l \frac{I_l}{N_l M_l} \sum_j \tilde{\varepsilon}_{\nu,\vec{q}}(l,j) \otimes \tilde{\varepsilon}_{\nu,\vec{q}}^*(l,j). \quad (19)$$

In the case of a monolayer alkali atoms adsorbed on, e.g., Cu(111), the deformation potential is different within the alkali layer compared to within the copper layers. In this case,  $V_d$  is to be interpreted as a fitted effective deformation potential of the system.

We have presented an approximative scheme to obtain ESF of a surface-localized electronic state. The input is the phonon structure, dispersion relation  $\omega_{\nu,\vec{q}}$  and polarization vector field  $\tilde{\varepsilon}_{\nu,\vec{q}}$ , and the surface-state wave function  $\psi_{ss}$ . With this input data we obtain the ESF, except for a multiplicative factor  $V_d^2$  [Eq. (19)].

For the application of this scheme to estimate the phonon-induced lifetime broadening, we proceed in two steps. First, we determine the single parameter of the model  $V_d^2$  by fitting the experimentally determined  $\lambda_0$  with the result in Eq. (5) with the ESF given by Eq. (11), where the  $B$  function is given by Eq. (19). Second, we apply Eq. (2) to obtain the lifetime broadening.

We still have a parametrized model for the ESF as the Debye models. However, the advantage with our scheme is that we have only one single fitting parameter, corresponding

to the effective deformation potential. Furthermore, we include the essential details, which determine the strength of the EP coupling, the wave function of the surface-localized electron state, and the full phonon structure of the system.

In Sec. II, we test our approximative scheme outlined above by comparing with previous calculations for some systems. We find that the approximation is sound and gives reasonable results. As we apply a fitting procedure with experimental data to determine  $V_d^2$ , we regard the obtained value of the  $V_d$  as an effective deformation potential with respect to all contributing initial  $\vec{k}$  states. Thus, even if the initial states deviate from a complete set within the volume spanned by the deformation potential, the approach makes sense.

### III. CALCULATION

Prior to presenting some results, applying our scheme, we describe in this section a model calculation of electronic wave functions and phonon structure needed for the calculation of the ESF. It should be noted here that we, as many other groups today are in the position to do this ground state calculation of the electronic and phonon structures from the *first principles*, applying, e.g., DFT and density-functional perturbation theory (DFPT) based calculations, respectively. However, the aim here is to present a simpler scheme for the calculation of ESF, in order to obtain information about the EP coupling for more complex systems. Thus, it is reasonable to illustrate the applicability with some model calculations.

#### A. Electronic structure

The adsorption structures from low to high cesium monolayer coverages have been investigated in a recent STM experiments.<sup>29</sup> At a low coverage  $\theta=0.05$ , a  $(\sqrt{19} \times \sqrt{19})R23.4^\circ$  structure is found. At intermediate Cs coverage on Cu(111), incommensurate hexagonal structures rotate somewhat relative to the substrate structure. Then a  $p(2 \times 2)$  structure is formed at  $\theta=0.25$ , where the Cs atoms sit at on-top site, which has been reported in some previous studies.<sup>11,12,30,31</sup> For the  $p(2 \times 2)$  structure, the electronic structure and electron dynamics have been studied in detail with STS and PES.<sup>11,12</sup> These studies showed the existence of the QWS close to the Fermi level in the  $\bar{\Gamma}$  point, and recent DFT calculations have predicted the existence of the GS.<sup>25</sup>

The electronic wave function of the QWS of  $p(2 \times 2)$ , Cs/Cu(111) is obtained from the model potential proposed by Lindgren *et al.*<sup>32</sup> The one-dimensional potential consists of three parts, the Cu (bulk) part ( $z \leq 0$ ),

$$V(z) = V_0 - 2V_g \cos(gz), \quad (20)$$

where  $g$  is the reciprocal-lattice vector, the Cs part ( $0 \leq z \leq d$ ),

$$V(z) = E_s, \quad (21)$$

where  $E_s$  is a constant discussed below, and finally the image potential ( $d \leq z$ ),

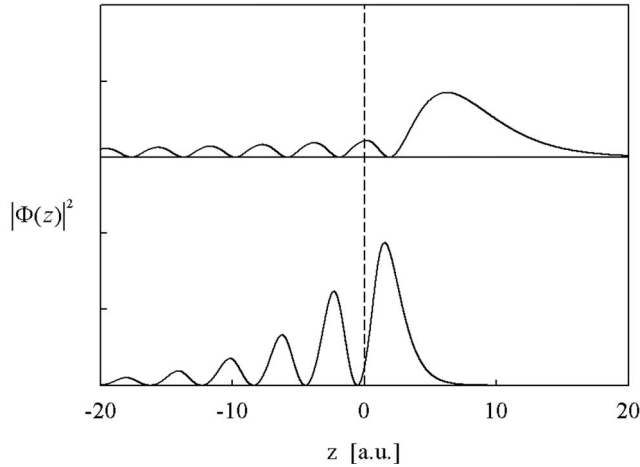


FIG. 1. Squared magnitude of wave functions in the  $\bar{\Gamma}$  point of a clean Cu(111). Upper figure: Image state (IS). Lower figure: Surface state (SS). The vertical dashed line indicates the position of the topmost layer of copper atoms.

$$V(z) = -\frac{1}{4(z - z_{im})}. \quad (22)$$

For the copper part, the energy parameters of the potential are obtained from Ref. 33. The authors constructed the potential to reproduce the wave functions obtained from the *first-principles* calculation, including the energy position of IS in clean metal surfaces.

The work function of a clean Cu(111) surface is 4.85 eV (Ref. 34). When the  $p(2 \times 2)$  monolayer of Cs is adsorbed at ( $\theta=0.25$ ), the work function decreases with  $\sim 3.0$  eV (Ref. 35). To include this effect, we shift the potential of Cu upward by the work function change. For the Cs part of the potential, a constant is used,  $E_s$ . The width of this part of the potential  $d$  is assumed to be 4.71 Å. The calculated wave functions are shown to be insensitive to changes of  $d$  by  $\pm 0.1$  Å.

The position of the image plane is determined by the requirement that the image potential should take the value of  $E_s$  at  $z=d$ . Thus the only fitting parameter here is  $E_s$ . The value of this parameter is set to fit the experimental energy eigenvalue of the QWS in the  $\bar{\Gamma}$  point measured by a PES, and calculated from the *first principles*.<sup>11</sup>

The calculated wave functions of the image and SSs of Cu(111) are shown in Fig. 1, and of the Gs and QWS in good agreement with the *first-principles* calculation<sup>11</sup> in Fig. 2. The wave function of GS is obtained from Ref. 25.

## B. Phonon structure

The phonon structure is determined by taking into account only the nearest-neighbor central force of Cu-Cu, Cu-Cs, and Cs-Cs. For the force constant of Cu-Cu, we use the parameter 27 N/m proposed by Black *et al.*<sup>36,37</sup> With this parameter, the phonon-dispersion relations of a clean Cu(111) surface agrees well with the data from He-atom scattering experiments. Our calculated phonon-dispersion relation for

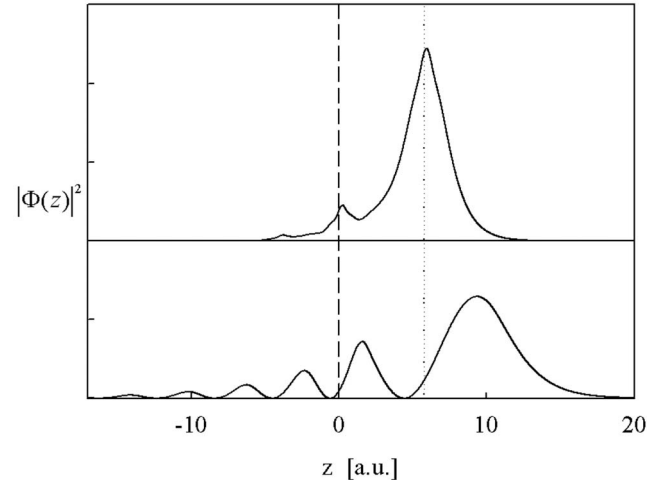


FIG. 2. Squared magnitude of wave functions in the  $\bar{\Gamma}$  point of Cs/Cu(111). Upper figure: Gap state (GS). Lower figure: Quantum-well state (QWS). The vertical dashed and dotted lines indicate the positions of the topmost layer of copper atoms and cesium atoms, respectively.

the clean Cu(111) surface is shown for a  $(1 \times 1)$  and  $p(2 \times 2)$  unit cell in Figs. 3 and 4, respectively.

When the  $p(2 \times 2)$  Cs overlayer is adsorbed on the Cu surface, we have backfolding bands due to the change of periodicity. The Brillouin zone, as well as the notation of high-symmetry points for the  $p(2 \times 2)$  structure are shown in Fig. 5. Note that for the  $p(2 \times 2)$  zone, the  $(1 \times 1)$   $\bar{M}$  point is equivalent to  $\bar{\Gamma}$ , and in the middle between the pictured  $\bar{K}'$  and  $\bar{K}$ , a  $\bar{M}'$  point appears.

The phonon-dispersion relation of a clean Cu(111)- $(2 \times 2)$  structure obtained by single force-constant method along the high-symmetry points is shown in Fig. 4.

The force constant of Cu-Cs is determined from a DFT calculation, applying the VASP code,<sup>38-40</sup> displacing the Cs atom 0.1 Å normal to the surface. We obtained a value of 32 N/m for the force constant. For the Cs-Cs force constant, we take the value of bulk Cs, 2.2 N/m (Ref. 18).

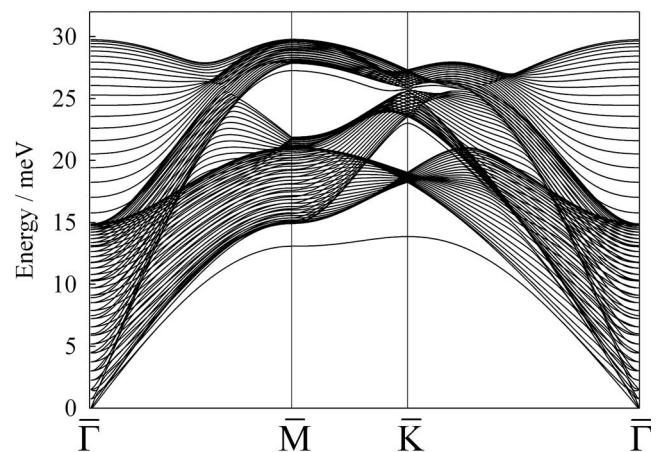


FIG. 3. The phonon-dispersion relation of Cu(111) for a  $(1 \times 1)$  unit cell, obtained by the single force-constant model (Refs. 36 and 37).

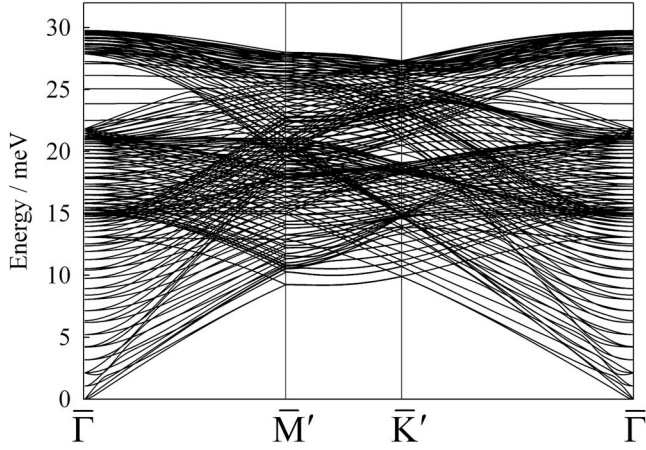


FIG. 4. The phonon-dispersion relation of Cu(111) for a  $p(2 \times 2)$  unit cell, obtained by the single force-constant model (Refs. 36 and 37).

The three force constants, Cu-Cu (27 N/m), Cu-Cs (32 N/m), and Cs-Cs (2.2 N/m) determine the dynamical matrix. Diagonalizing the dynamical matrix for each  $q$  point, we obtain phonon frequencies and polarization vector fields for each mode. The obtained phonon-dispersion relation is shown in Fig. 6.

The prominent difference from the clean Cu surface is the appearance of three low-frequency Cs-induced phonon modes below the bulk bands. These modes are consistent with the He atom scattering experimental results of similar system Cs/Cu(001) (Ref. 18). Two of the three Cs modes are attributed to the pure in-plane polarization, and the highest energy mode to polarization normal to the surface. The phonon density of states projected on different atomic layers are shown in Fig. 7. In the left part of the figure [Cu(111)], the two peaks 13 meV and 27 meV, clearly seen in the surface plane ( $S$ ), refer to the surface Rayleigh mode polarized normal to the surface and the longitudinal gap mode polarized in-plane (see Fig. 3 in the  $\bar{M}$  point). The right hand side of Fig. 7 shows in the upper panel, the Cs-localized phonon modes Cs/Cu(111).

IV. LIFETIME BROADENING

In this section we will present some results of the calculated phonon-induced lifetime broadening, applying our

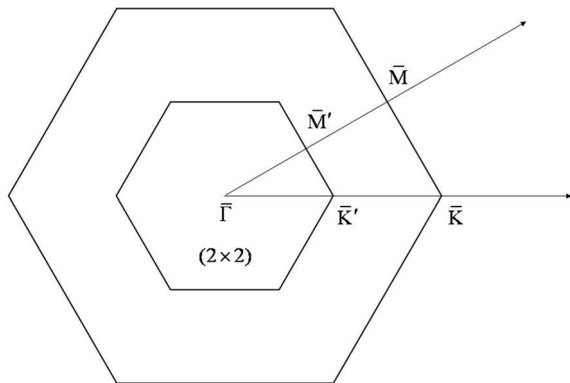


FIG. 5. Surface-Brillouin zone of (outer hexagon) a clean Cu(111) and inner hexagon  $p(2 \times 2)$ -Cs/Cu(111).

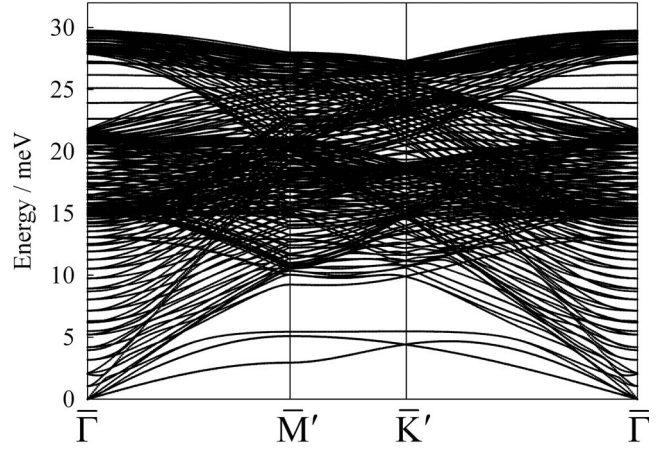


FIG. 6. Phonon-dispersion relation for the  $p(2 \times 2)$ -Cs/Cu(111) surface.

scheme for the ESF. The results are summarized in Table I. We first consider the SS and the lowest lying IS of the clean Cu(111) surface. The calculated ESF for these states are shown in Fig. 8. We can regard the ESF as the phonon-density of states weighted by the EP coupling [see Eq. (11)]. The phonon-density of states is determined by the dispersion relation in Fig. 3, and the EP coupling is to a large extent,

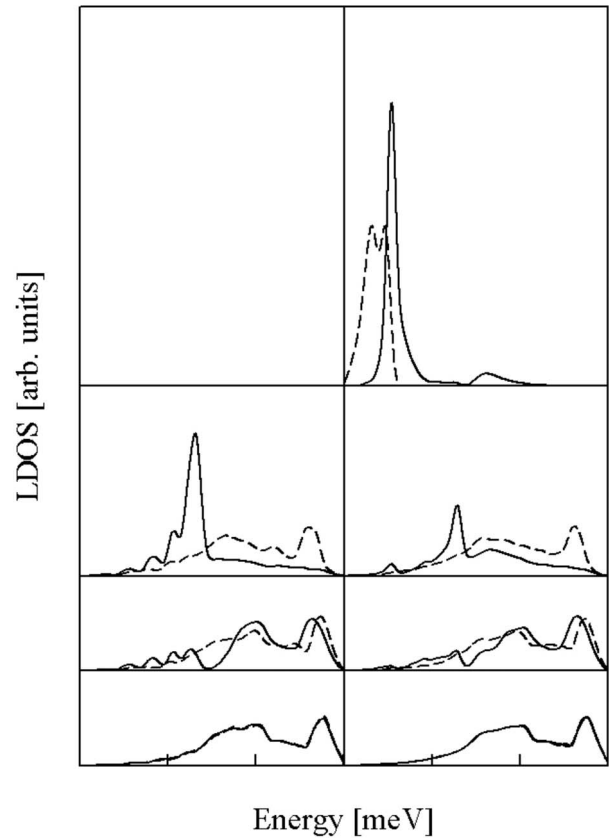


FIG. 7. Projected density of phonon states of Cu(111), shown in the left panels and Cs/Cu(111), shown in the right panels.  $z$  polarized (solid line) and in-surface plane polarized (dashed line). Top figure: first layer, middle panel: second layer, and bottom panel: third layer.

TABLE I. Electron-phonon coupling constant  $\lambda_0$  at  $T=0$  and the phonon-induced lifetime broadening  $\Gamma$ . The references denoted [\*] are results of the present calculations.

State		$\lambda_0$	$\Gamma$ [meV]
SS	[*]	0.14	5.5
	Ref. 42	0.16	6.9
IS	[*]	0.05	2.3
	Ref. 43	0.06	
QWS	[*]	0.18	3.3
	Ref. 11		7.0
	Ref. 12		7.5
GS	[*]	0.28	4.6

determined by the overlap between the phonon-displacement fields and the spatial distribution of the electron wave function of the surface or IS shown in Fig. 1.

The two major peaks in the ESF in Fig. 8 at about 13 and 27 meV, reflect high phonon-density of states due to the flat dispersion of the surface-localized Rayleigh and gap-phonon mode, respectively, in the  $\bar{M}$  point. The intensity in the region between 15 and 22 meV is due to the high density of bulk phonon states. Due to the fact that the wave functions of the surface and IS have a substantial weight at the surface (in particular the SS), the contribution from the surface-phonon modes to the ESF will be enhanced.

The parameter  $V_d^2$  in Eq. (19) is determined to reproduce the experimentally determined  $\lambda_0$  value 0.14.<sup>41,43</sup>

We next integrate the ESF to obtain the phonon-induced lifetime broadening for the SS, with the result  $\Gamma=5.5$  meV. This result is in fair agreement with the calculation of  $\lambda_0=0.16$  and  $\Gamma=6.9$  meV by Eiguren *et al.*<sup>42</sup> In Ref. 42 the phonon and electron structures are calculated in a similar fashion as in the present work. However, the deformation potential calculation, based on a screened Ashcroft potential is done explicitly. With the parameter  $V_d^2$  we obtained for the SS, we used to determine  $\lambda_0=0.05$  and  $\Gamma=2.3$  meV for the IS of Cu(111). Time-resolved photoemission spectroscopy

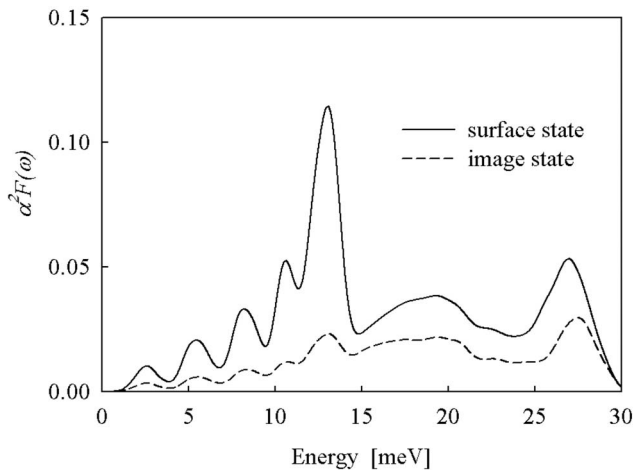


FIG. 8. Eliashberg spectral functions for the SS (solid line) and IS (dashed line) of Cu(111).

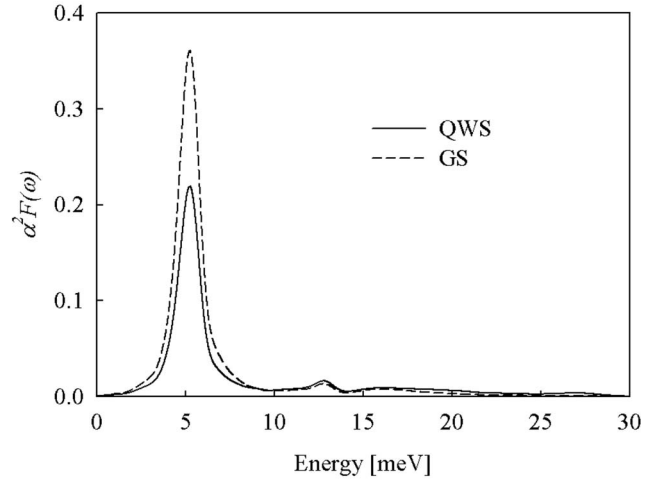


FIG. 9. ESFs of the QWS and the GS.

measurements by E. Knoesel and coworkers<sup>43</sup> gave  $\lambda_0=0.06 \pm 0.01$  for the IS of Cu(111), which agrees well with our value.

We have furthermore calculated the phonon-induced lifetime broadening of the two previously discussed surface-localized states of  $p(2 \times 2)$ -Cs/Cu(111), the QWS, and the GS. The corresponding two ESFs are shown in Fig. 9, respectively.

The feature around 5 meV is ascribed to the Cs-induced phonon modes shown in Fig. 7. It is obvious that these modes play a crucial role in the phonon-induced lifetime broadening in this system.

With the Eliashberg function for the QWS and the recently determined experimental  $\lambda_0$  parameter of 0.18 in a photoemission experiment,<sup>11</sup> we calculate the lifetime broadening  $\Gamma=3.3$  meV. In the previous 2D and 3D Debye model calculations,  $\Gamma=7.5 \pm 3.0$  meV (Ref. 12) and 7.0 meV (Ref. 11) are obtained. The larger values of  $\Gamma$  applying the Debye models can be explained as follows: From Eqs. (2) and (5) the difference of  $\Gamma$  and  $\lambda_0$  is the factor  $1/\omega$  in the integrand. So, fitting to a given  $\lambda_0$  value, the factor  $V_d^2$  becomes small when we have major contributions from low-frequency phonon modes. As the details of both the phonon and electron structures are missing in Debye-model-based calculations, we believe our estimates are more reliable.

We finally calculate the lifetime broadening of the GS of Cs/Cu(111) with the same effective deformation potential as for the QWS. The  $\lambda_0$  value obtained is 0.28 and  $\Gamma=4.6$  meV. It is interesting to note that even though the GS is much more decoupled from the copper substrate than the QWS (see Fig. 2),  $\Gamma$  is greater (see Table I). This somewhat surprising result is due to a larger real-space overlap with low-frequency Cs-phonon modes, which is clearly seen in Fig. 7.

## V. SUMMARY

In summary, we have developed an approximative procedure for calculations of the phonon-induced lifetime broadening of surface electronic states. The aim has been to de-

velop a semiempirical scheme, which is more appropriate than simple Debye models but less cumbersome than the *first-principles* methods. This is in particular, important when considering more complex systems, such as, e.g., overlayer systems. Full *first-principles* calculations of phonon-induced lifetime broadening of electronic states exist today only for bulk, clean surfaces and unsupported atomic layers. The Eliashberg function includes a multiplicative fitting parameter, representing the square of the effective deformation potential, and in addition the electron and phonon structures of desired quality.

In this work we analyze the surface and ISs of a clean Cu(111), and QWS and GS of  $p(2 \times 2)$ -Cs/Cu(111). We show that the calculated EP-induced lifetime broadening of these states agrees reasonably with previous calculations. However, compared to calculations based on Debye phonon models, our line widths are substantially smaller, almost a factor of two. These results reflect the fact that information of, in particular, surface phonon modes is important. The low lying Cs-induced phonon modes play a crucial role in determining the line width of the QWS and the GS of Cs/Cu(111).

## APPENDIX

In this Appendix, we derive the renormalized polarization vector,

$$\vec{\tilde{\epsilon}}(\nu\vec{q}) = [\tilde{\epsilon}_x(\nu\vec{q}), \tilde{\epsilon}_y(\nu\vec{q}), \epsilon_z(\nu\vec{q})], \quad (\text{A1})$$

where

$$\tilde{\epsilon}_x = i \frac{q_x}{k_0} \epsilon_x, \quad \tilde{\epsilon}_y = i \frac{q_y}{k_0} \epsilon_y, \quad (\text{A2})$$

and  $k_0$  is the Thomas-Fermi wave vector given by

$$k_0 = \left( \frac{12}{\pi} \right)^{1/3} r_s^{-1/2} a.u., \quad (\text{A3})$$

where  $r_s$  is the free-electron density parameter in atomic units (AU), defined by the electron density  $\rho$  by the relation ( $\rho^{-1} = \frac{4\pi}{3} r_s^3$ ). The details of this approximation are as follows:

We assume the free-electron dispersion of electron states parallel to the surface (in  $x$  and  $y$  plane). Let's consider the  $x$  component of the EP matrix element in Eq. (8). Partial integration in the  $(x, y)$  plane gives

$$\langle ss | \epsilon_x \frac{\partial V}{\partial x} | \vec{k} \rangle = i q_x \langle ss | \epsilon_x V | \vec{k} \rangle, \quad (\text{A4})$$

we rewrite this in the following way:

$$\langle ss | \epsilon_x V | \vec{k} \rangle = \langle ss | \epsilon_x \left( \frac{\partial V}{\partial z} \right)^{-1} \frac{\partial V}{\partial z} | \vec{k} \rangle = \langle ss | \epsilon_x \left( \frac{\partial}{\partial z} \ln V \right)^{-1} \frac{\partial V}{\partial z} | \vec{k} \rangle. \quad (\text{A5})$$

If we assume that the screened attractive electronion potential  $V$  has an exponential decay constant, given by the Thomas-Fermi wave vector  $k_0$  (see Appendix B in Ref. 44), we have

$$\frac{\partial}{\partial z} \ln V = k_0. \quad (\text{A6})$$

Thus, we may express the deformation potential with respect to the displacement in  $x$ ,  $y$ , and  $z$  in terms of only the partial derivative with respect to the  $z$  coordinate,

$$\langle ss | \epsilon_x \frac{\partial V}{\partial x} | \vec{k} \rangle \approx i \frac{q_x}{k_0} \langle ss | \epsilon_x \frac{\partial V}{\partial z} | \vec{k} \rangle = \langle ss | \tilde{\epsilon}_x \frac{\partial V}{\partial z} | \vec{k} \rangle. \quad (\text{A7})$$

For the  $y$  component, we then have

$$\langle ss | \epsilon_y \frac{\partial V}{\partial y} | \vec{k} \rangle \approx i \frac{q_y}{k_0} \langle ss | \epsilon_y \frac{\partial V}{\partial z} | \vec{k} \rangle = \langle ss | \tilde{\epsilon}_y \frac{\partial V}{\partial z} | \vec{k} \rangle. \quad (\text{A8})$$

- <sup>1</sup>R. D. Diehl and R. McGrath, Surf. Sci. Rep. **23**, 43 (1996).
- <sup>2</sup>S.-Å. Lindgren and L. Walldén, Solid State Commun. **34**, 671 (1980).
- <sup>3</sup>S.-Å. Lindgren and L. Walldén, Phys. Rev. Lett. **59**, 3003 (1987).
- <sup>4</sup>A. Carlsson, D. Claesson, S.-Å. Lindgren, and L. Walldén, Phys. Rev. B **52**, 11144 (1995).
- <sup>5</sup>A. Carlsson, D. Claesson, G. Katrich, S.-Å. Lindgren, and L. Walldén, Surf. Sci. **352**, 656 (1996).
- <sup>6</sup>A. Carlsson, B. Hellsing, S.-Å. Lindgren, and L. Walldén, Phys. Rev. B **56**, 1593 (1997).
- <sup>7</sup>A. Carlsson, D. Claesson, G. Katrich, S.-Å. Lindgren, and L. Walldén, Phys. Rev. B **57**, 13192 (1998).
- <sup>8</sup>J. M. Carlsson and B. Hellsing, Phys. Rev. B **61**, 13973 (2000).
- <sup>9</sup>B. Hellsing, J. Carlsson, L. Walldén, and S.-Å. Lindgren, Phys. Rev. B **61**, 2343 (2000).
- <sup>10</sup>E. V. Chulkov, J. Kliewer, R. Berndt, V. M. Silkin, B. Hellsing, S. Crampin, and P. M. Echenique, Phys. Rev. B **68**, 195422 (2003).

- <sup>11</sup>M. Breitholtz, V. Chis, B. Hellsing, S.-Å. Lindgren, and L. Walldén, Phys. Rev. B **75**, 155403 (2007).
- <sup>12</sup>C. Corriol, V. M. Silkin, D. Sanchez-Portal, A. Arnau, E. V. Chulkov, P. M. Echenique, T. von Hofe, J. Kliewer, J. Kroger, and R. Berndt, Phys. Rev. Lett. **95**, 176802 (2005).
- <sup>13</sup>S.-Å. Lindgren, C. Svensson, and L. Walldén, Phys. Rev. B **42**, 1467 (1990).
- <sup>14</sup>C. Astaldi, P. Rudolf, and S. Modesti, Solid State Commun. **75**, 647 (1990).
- <sup>15</sup>P. Rudolf, C. Astaldi, G. Gautero, and S. Modesti, Surf. Sci. **251/252**, 127 (1991).
- <sup>16</sup>G. Benedek, J. Ellis, A. Reichmuth, P. Ruggerone, H. Schief, and J. P. Toennies, Phys. Rev. Lett. **69**, 2951 (1992).
- <sup>17</sup>S.-Å. Lindgren, C. Svensson, and L. Walldén, J. Electron Spectrosc. Relat. Phenom. **64/65**, 483 (1993).
- <sup>18</sup>G. Witte and J. P. Toennies, Phys. Rev. B **62**, R7771 (2000).
- <sup>19</sup>S. Baroni, S. de Gironcoli, A. Dal Corso, and P. Giannozzi, Rev. Mod. Phys. **73**, 515 (2001).
- <sup>20</sup>A. Eiguren, S. de Gironcoli, E. V. Chulkov, P. M. Echenique, and

- E. Tosatti, Phys. Rev. Lett. **91**, 166803 (2003).
- <sup>21</sup>I. Y. Sklyadneva, E. V. Chulkov, P. M. Echenique, and A. Eiguren, Surf. Sci. **600**, 3792 (2006).
- <sup>22</sup>A. Leonardo, I. Y. Sklyadneva, P. M. Echenique, and E. V. Chulkov, Surf. Sci. **600**, 3715 (2006).
- <sup>23</sup>A. Leonardo, I. Y. Sklyadneva, V. M. Silkin, P. M. Echenique, and E. V. Chulkov, Phys. Rev. B **76**, 035404 (2007).
- <sup>24</sup>I. Y. Sklyadneva, A. Leonardo, P. M. Echenique, and E. V. Chulkov, Surf. Sci. **601**, 4022 (2006).
- <sup>25</sup>V. Chis, S. Caravati, G. Butti, M. I. Trioni, P. Cabrera-Sanfeliu, A. Arnau, and B. Hellsing, Phys. Rev. B **76**, 153404 (2007).
- <sup>26</sup>G. Grimvall, in *The Electron-Phonon Interaction in Metals*, edited by E. Wohlfarth, Selected Topics in Solid State Physics (North-Holland, New York, 1981).
- <sup>27</sup>B. Hellsing, A. Eiguren, and E. V. Chulkov, J. Phys.: Condens. Matter **14**, 5959 (2002).
- <sup>28</sup>A. Nojima, K. Yamashita, and B. Hellsing, J. Phys.: Condens. Matter **20**, 224018 (2008).
- <sup>29</sup>Th. von Hofe, J. Kroger, and R. Berndt, Phys. Rev. B **73**, 245434 (2006).
- <sup>30</sup>S.-Å. Lindgren, L. Walldén, J. Rundgren, P. Westrin, and J. Neve, Phys. Rev. B **28**, 6707 (1983).
- <sup>31</sup>W. C. Fan and A. Ignatiev, J. Vac. Sci. Technol. A **6**, 735 (1988).
- <sup>32</sup>S.-Å. Lindgren and L. Walldén, Phys. Rev. B **38**, 10044 (1988).
- <sup>33</sup>E. V. Chulkov, V. M. Silkin, and P. M. Echenique, Surf. Sci. **437**, 330 (1999).
- <sup>34</sup>P. O. Gartland and B. J. Slagsvold, Phys. Rev. B **12**, 4047 (1975).
- <sup>35</sup>S.-Å. Lindgren and L. Walldén, Solid State Commun. **25**, 13 (1978).
- <sup>36</sup>J. E. Black, F. C. Shanes, and R. F. Wallis, Surf. Sci. **115**, 161 (1982).
- <sup>37</sup>J. E. Black, D. A. Campbell, and R. F. Wallis, Surf. Sci. **133**, 199 (1983).
- <sup>38</sup>G. Kresse and D. Joubert, Phys. Rev. B **59**, 1758 (1999).
- <sup>39</sup>G. Kresse and J. Furthmüller, Comput. Mater. Sci. **6**, 15 (1996).
- <sup>40</sup>G. Kresse and J. Furthmüller, Phys. Rev. B **54**, 11169 (1996).
- <sup>41</sup>B. A. McDougall, T. Balasubramanian, and E. Jensen, Phys. Rev. B **51**, 13891 (1995).
- <sup>42</sup>A. Eiguren, B. Hellsing, F. Reinert, G. Nicolay, E. V. Chulkov, V. M. Silkin, S. Hufner, and P. M. Echenique, Phys. Rev. Lett. **88**, 066805 (2002).
- <sup>43</sup>E. Knoesel, A. Hotzel, M. Wolf, and J. Electronspec, J. Electron Spectrosc. Relat. Phenom. **88-91**, 577 (1998).
- <sup>44</sup>A. Eiguren, B. Hellsing, E. V. Chulkov, and P. M. Echenique, Phys. Rev. B **67**, 235423 (2003).